Zeitschrift: IABSE congress report = Rapport du congrès AIPC = IVBH Kongressbericht

Band: 6 (1960)

Rubrik: Ia. Properties of materials

Ia1

Laboratory Testing of Full-size Aluminum Bridge

Essais de laboratoire en vraie grandeur sur un pont en aluminium

Laboratoriumversuche an einer Aluminiumbrücke in voller Größe

JAMES MICHALOS, Ph. D., Prof. and Chairman
GERALD G. KUBO, Ph. D., Associate Professor
CHARLES BIRNSTIEL, M.C.E., Instructor
Department of Civil Engineering, New York University, New York, N. Y., U.S.A.

Introduction

Under sponsorship of the Reynolds Metals Company, two general types of tests were performed at New York University on a 60-ft. prototype aluminum bridge with concrete floor slab, as follows:

1. Static-load tests with loads producing maximum shears and moments equal to 1 and 2 times design values for the H 20 loading of the American Association of State Highway Officials (AASHO).
2. Repeated-load tests with loads producing maximum moments equal to 1 and $1^1/_2$ times design values for H 20 loading.

In addition, the natural frequency of the bridge was determined experimentally.

The purpose of the tests was to investigate the structural suitability of the bridge for the service for which it was designed. This was accomplished by visual observation as well as by strain and deflection measurements. These tests were a first step in a long-range development program, and the results are being used for improving highway bridge designs on which the Reynolds Metals Co. is working.

Description of Test Bridge

The test bridge (see Fig. 1 and Fig. 2) had three prefabricated, aluminum modular units supported on commercial type (Lubrite) bearings which rested on concrete piers founded on rock. The reinforced concrete slab was, on the

average, slightly over $6^1/_2$-in. thick. It was joined to the aluminum modules by means of extruded aluminum shear transfer devices in order to insure composite action. The Z-shape shear devices are shown in place during erection in Fig. 3. All aluminum components were fabricated from a non heat-treatable

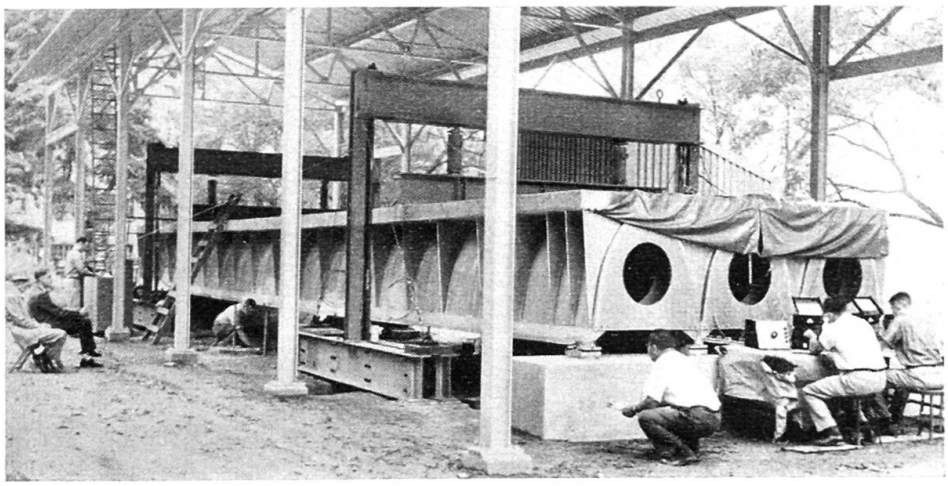

Fig. 1. Static Load Test.

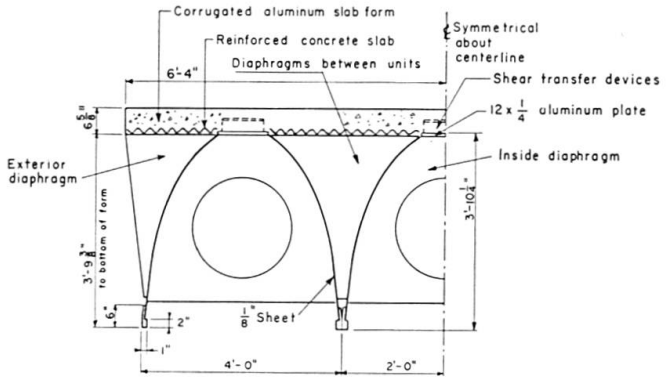

Fig. 2. Half-Section Through Bridge.

aluminum-magnesium alloy designated as 5083. The shear devices and the extrusions which formed the bottom flanges were cold work-hardened to H 112 temper. All other components were made from annealed metal (0 temper).

Each modular unit consisted of curved, $^1/_8$-in. thick, side sheets welded to the bottom extrusions and to a 12-in. wide by $^1/_4$-in. thick plate at the top. A unit had nine inside diaphragms, of $^1/_4$-in. thick plate, connected to it by Huck fasteners. Two of these were over each end bearing and five at intermediate points. Other $^1/_4$-in. diaphragms, more closely spaced, were installed between adjoining units and on the outer side of the exterior units. Adjoining bottom extrusions were bolted together by means of $^1/_4$-in. high strength bolts spaced at 10-in. centers.

Loads were applied to the test bridge by hydraulic rams reacting against structural steel yokes which transferred the ram reactions to anchor rods embedded in rock. Fig. 1 shows the loading yokes in place for a static load test.

Instrumentation

The instrumentation was planned in accordance with the stated purpose, which was to conduct static and repeated-load tests, and to record a limited number of strain and deflection measurements. Vertical deflections of the test

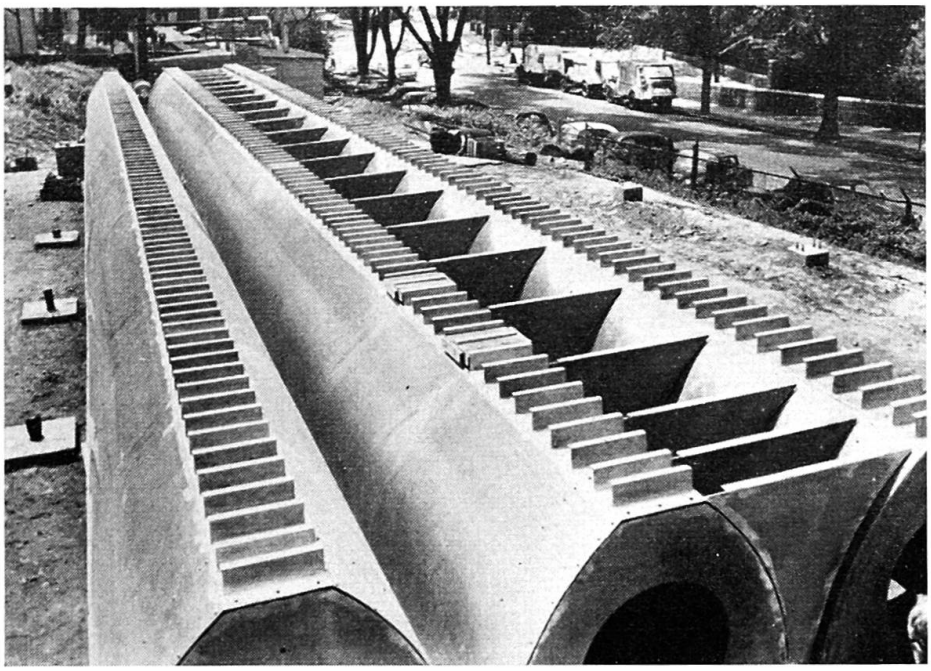

Fig. 3. View During Erection.

bridge were determined by means of a Wild N 2 Level, and longitudinal movements at the expansion end of the test bridge were observed by means of dial gages. Transverse horizontal movements of the bottom extrusions were determined by using plumb bobs hung from the extrusions; but, as maximum transverse movements during the first static tests were on the order of one millimeter, these measurements were discontinued for all subsequent tests.

Strains produced in the test structure by the weight of the concrete slab and by static and repeated loads were measured at selected points by means of Baldwin SR-4 electrical resistance strain gages placed in both uniaxial and rosette patterns. The leads from the gages were wired to switching units, and Baldwin Strain Indicators were used to determine the change in strain corresponding to an increment of load. When the variation of strain with respect

to time was desired, as during the monitoring of the repeated-load tests, a strain gage was connected to a Brush Universal Analyzer and the data plotted on a Brush Paper Strip Recorder.

Static Load Tests

The following four types of static load tests were made:

1. Concrete slab on the aluminum modular units.
2. Two symmetrically applied loads on the composite structure, resulting in simultaneous design values, or multiples thereof, of bending moment and shear.
3. Eccentrically applied loads on the composite structure.
4. Single applied load at mid-span of the composite structure.

Concrete Slab on Aluminum Modular Units

To observe the behavior of the aluminum structure as the concrete was placed, selected gages and scales were monitored. The difference between the final and original sets of readings was considered as the effect of the weight of the concrete slab on the aluminum structure. A comparison between measured and computed deflections, and between measured and computed strains showed good correlation.

Two Symmetrically Applied Loads

The live loads were applied, as shown in Fig. 1, by means of hydraulic rams symmetrically positioned on transverse distribution beams. Thus the force was distributed essentially as a line load across the width of the deck. The loads were placed 12 ft. 2 in. from each end bearing so as to produce vertical shear and bending moment values which would be proportional to the design shear and design moment respectively. As used herein, design shear and design moment are the maximum values produced in a one-lane, simply-supported bridge by a 20-ton truck, together with impact effect, as defined by the current AASHO specifications.

Computed theoretical values of deflections, stresses, and longitudinal movements were based on the following assumptions:

1. There was complete composite action between the concrete slab and the aluminum structure (the ratio of modulus of elasticity of aluminum to that of concrete was taken as 3.5).
2. The load applied through the distribution beam was shared equally by the three modular units.

Fig. 4 shows the vertical deflection at the centerline of the span as the load was increased to 2 times design value and then removed. The plotted values, obtained by averaging the measured deflections at the four lines of extrusions, define reasonably smooth curves during the loading and unloading stages. Up to approximately 1.5 times design load the measured deflections varied almost linearly with load but lagged in comparison to the computed

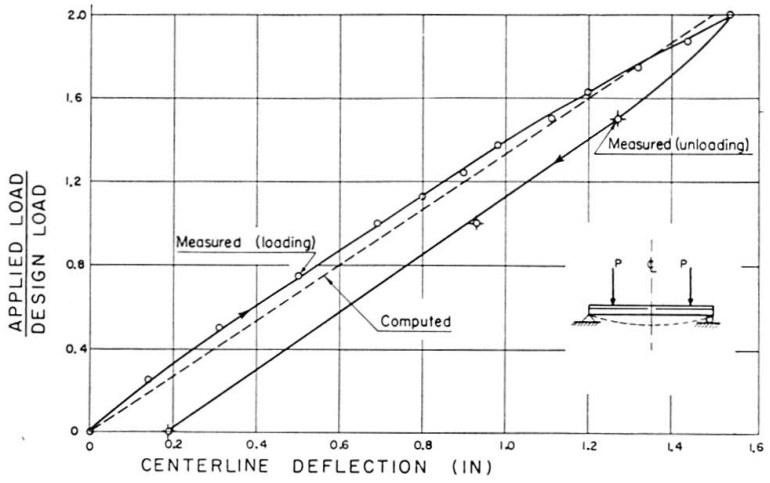

Fig. 4. Centerline Deflection.

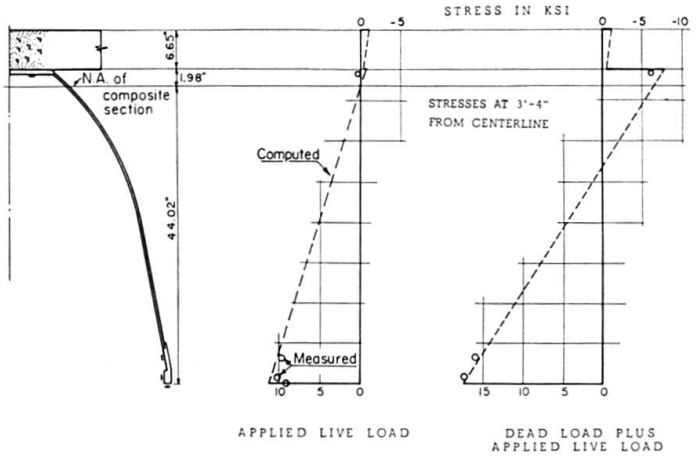

Fig. 5. Stresses at Two Times Design Moment.

values. At loads above 1.5 times design value, the deflections increased non-linearly with load so that at the maximum of 2.0 times design value the measured vertical deflection was slightly larger than the computed value. As reported subsequently, the lag in measured deflections was due principally to end bearing friction.

Comparison of measured with computed values of longitudinal movement showed good correlation, but with a lag of almost 10 percent in the measured values throughout the loading range. During the unloading stage the lag of measured movement was still more pronounced. As in the case of vertical

deflections, this was due principally to the frictional restraint of the sliding detail at the expansion end.

Computed bending stresses and those deduced from measured strains, in kips per sq. in., are shown in Fig. 5. In the bottom extrusion the measured values are consistently lower than the theoretical values, with a maximum difference of approximately 10 percent. The strain gage readings on the underside of the top plate, although somewhat erratic because of the very low level of stress, are consistent with the anticipated position of the neutral axis.

Some evidence of structural distress was observed as the applied load was increased from $1\,^7/_8$ to 2.0 times design moment and shear. There was some local yielding and buckling in the $^1/_8$-in. sheet over the supports. The buckles were of limited size ($^1/_{16}$-in.) and probably represented a readjustment of an unfavorable local condition.

Eccentrically Applied Loads

To make this test, only the hydraulic ram on the west portion of each of the two distribution beams was used to apply load. The measured deflections and stresses varied almost exactly linearly across the structure from a minimum value at the most easterly extrusion to a maximum value at the most westerly extrusion.

The primary objective of the static load tests was to study the over-all behavior of the test structure as reflected in changes in deflection and strains. The possibility of buckling of the curved sheets under load was recognized; however, due to the large number and variety of buckles in the structure as erected, no serious attempt was made to monitor all of the panels for new or modified buckles under applied load.

The three modular units, as received, contained a small number of large buckles in the curved sheets. After the erection of the modular units and the installation of the external diaphragms which divided the structure into 23 panels, additional buckles of varying size, shape and orientation were formed. A survey revealed that the six curved sheets contained as few as 3 buckles of noticeable size per sheet and as many as 22 per sheet. Although it was difficult to measure the size and amplitude of these distortions with any degree of accuracy, there were some which dished in or out as much as $^1/_2$ in.

Later, during the repeated-load program, it was noted that some of the buckled areas were "breathing". Apparently these buckles were straightening out elastically, under the effect of the diagonal tension stresses introduced by the applied load, moving back to their dead load configuration upon release of the load.

During the eccentric load test there occurred an incident that raised some questions regarding the stability of the panels under high shear loading. While readings were being taken under an eccentric load of $^7/_8$ of the design value,

an observer, leaning with his hand on a curved panel, produced a depression of approximately $^1/_2$ in. Apparently the buckled shape was stable, since no further change was detected as the load was increased to 1.0 times design load and then released.

Special Studies with Single Load at Mid-Span

During the repeated-load tests (discussed later), there were periods when cycling was suspended, and it was decided to utilize the loading set-up (single line-load at centerline) to investigate the effect of sliding friction at the bearing and the effect of using a line load rather than a simulated wheel concentration.

To study the effect of type of expansion bearing on deflection and on longitudinal movement, steel rollers on suitable bearing plates were substituted for the Lubrite plates. With roller supports the lag of measured values was eliminated. In addition, noises and jerky movements due to end restraint were essentially eliminated.

In all previous load tests a distribution beam, which rested on the roadway slab for its full width, had been placed under the ram. To simulate a wheel concentration, it was decided to use a steel plate. As it was inconvenient to remove the distribution beam, it was raised and the plate was placed between the beam and the roadway. There was no appreciable difference in behavior with the plate from what had been observed with the distribution beam.

Strains in the concrete slab were determined by means of suitably moisture-proofed SR-4 strain gages. Measured values were approximately 25 percent lower than computed values.

Repeated-Load Tests

After consultation with Mr. E. L. Erickson of the Bureau of Public Roads, the following program of repeated-load tests was adopted:

1. 50,000 cycles at 1.0 times design moment.
2. 750,000 cycles at 1.5 times design moment.

In all cases the load variation during cycling was from dead load to dead load plus live load. Load was applied by a single hydraulic ram acting on a distribution beam at mid-span.

Test Procedure

The hydraulic loading system was designed and built to apply a predetermined maximum force at the ram irrespective of any vertical movement of the bridge due to temperature change. Periodic checks and adjustments were made.

To provide a continuing check of the response of the structure, the operators monitored a selected group of strain gages, dial gages, and level targets. The readings were taken once each hour, and were followed immediately by a visual examination of the aluminum structure and the concrete deck for any signs of distress. After it became evident that fatigue was causing damage, greater emphasis was given to the visual inspection, and critical areas were kept under careful surveillance in order to detect cracks at an early stage of development.

Tests with Original Extrusions

The 50,000 cycles at 1.0 times design moment were completed without incident. After 360,595 cycles at 1.5 times design moment a crack was discovered. It had progressed through an interior bottom extrusion at mid-span and gone upward into the $^1/_8$-in. curved sheet for a distance of approximately 16 in., almost to the mid-height of the aluminum module. Fig. 6 is a photograph, with the interior diaphragm removed, showing the full extent of the crack. Note its progression through three holes in a vertical line, starting at the $^1/_4$-in. hole in the bottom extrusion.

A 6-in. wide section of the bottom extrusion and a 4-in. wide by $7\,^1/_2$-in. high portion of the curved sheet was cut out to remove the bulk of the crack. The balance of the crack in the sheet was enlarged with a saw after a hole

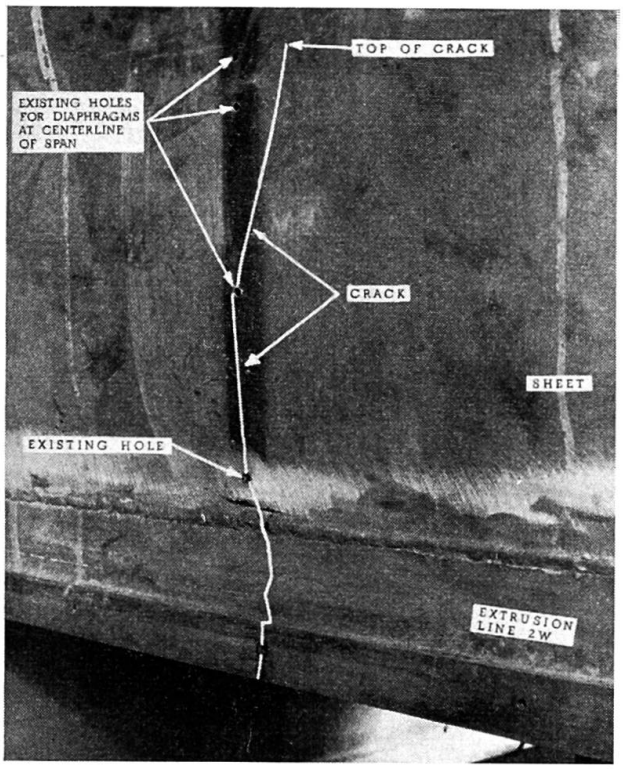

Fig. 6. Crack No. 1.

had been drilled at its upper extremity. Matching patch plates were prepared, positioned, and then welded using the inert gas shielded consumable-electrode process. The completed repair, with additional reinforcing plates for the bottom extrusion, is shown in Fig. 7. In order to replace the interior diaphragm that had been removed, portions of the weld seam were ground down.

Two other cracks, located within 20 in. of mid-span, were discovered before the sponsor decided to replace the bottom extrusions. The second crack occurred 47,045 cycles after the first and originated at a hole in another interior bottom

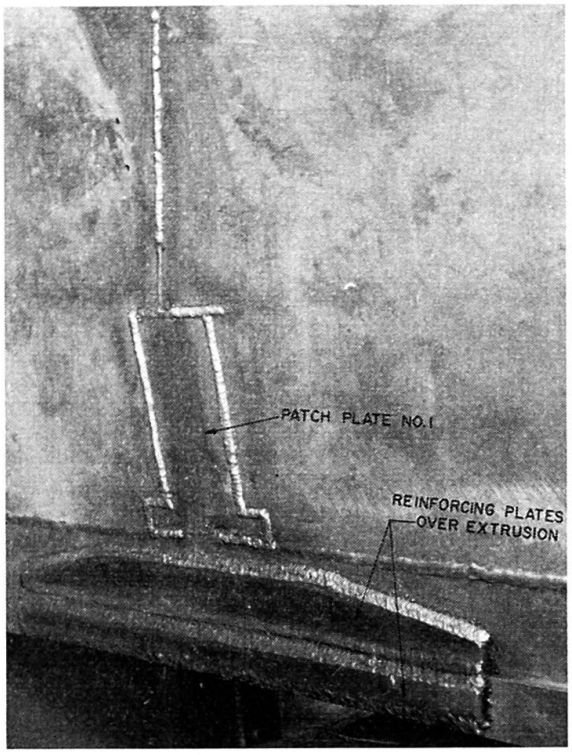

Fig. 7. Repair of Crack No. 1.

extrusion. It was repaired in a manner similar to that used for the first crack. In addition, 53 holes in the central portion of each extrusion were drilled to $^1/_2$-in. diameter and reamed. Of these holes, the 21 closest to mid-span were then plug welded. Due to the limited size of opening in proportion to depth, it was difficult to obtain full weld penetration. The third crack, working its way through a plug-welded hole in still another interior extrusion, forced a shut-down after an additional 39,760 cycles.

Tests with New Extrusions

After the third crack, the sponsor decided to discontinue the practice of making repairs as they became necessary and instead remove the central

49 ft. 6 in. of the bottom extrusions and replace them with others of a new design in which all holes were eliminated. Extrusions on interior lines were to be single units rather than pairs.

It was recognized that the test structure would then consist of two groups of parts with different loading histories. The new extrusions would have no history of repeated loads, while the remainder of the structure would have sustained 50,000 cycles at 1.0 times design moment and 447,000 cycles at 1.5 times design moment. In addition, there would be various difficulties involved in making such a major repair, but nonetheless the sponsor considered it preferable to replace the extrusions. A new extrusion is shown in Fig. 8 adjacent to the pair of extrusions it replaced.

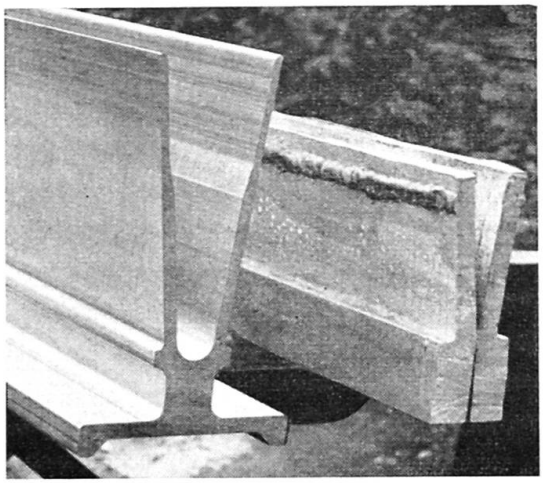

Fig. 8. New and Original Extrusions.

The plan was to raise the structure so as to relieve a designated portion of the dead load bending stresses in the structure, make the repair, and then restore essentially the same dead load stress conditions into the modified structure by removing the lifting force. The particular scheme devised incorporated an arrangement which, in order to keep the working area under the bridge as clear as possible, would permit lifting from above rather than pushing from below. Six $1\,^1/_4$-in. holes, three on each of two transverse lines, were drilled through the concrete slab and the top aluminum plates in order to insert hanger rods. Two banks of three hydraulic rams each were arranged so that lifting loads could be applied gradually to the structure along the two transverse lines.

The edges of the curved sheets took an irregular sinusoidal shape in the transverse direction when the extrusions were removed by sawing. They were eventually straightened out when the replacement section was fitted up and welded. Attention is called to the fact that the sawed edges were not ground smooth.

On the exterior lines, the lapped joint between the sheet and the extrusion was exposed so that both seams were accessible. A continuous fillet weld was made along the top of the extrusion. Later, to eliminate the possibility of cracks starting at the cut edge of the sheet, it was decided to join the lower edge of the plate to the side of the new extrusion by means of a similar weld. Along the interior lines, the rough edges of the sheets were inaccessible and could not be welded. Furthermore, since these edges were behind the stems of the new extrusions, they were hidden from view.

The junctions between new and existing extrusions were spliced using a combination of butt welds and strap plates. Rather large distortions were observed on the curved sheets of the panels in which the splices were made. However, except for some minor crater cracks in the welds, the splices and the affected sheets showed no signs of distress during the balance of the repeated load tests.

Before the additional 302,600 cycles required to complete the program were applied, it was necessary to stop testing six more times in order to repair cracks which developed. These were all located on one line near mid-span, in the vicinity of the longitudinal weld seam.

Analysis of the cracks indicates that they can be classified into two types. The first type is a crack in the weld seam of a previous repair and is due to a variety of reasons, including lack of penetration, removal of weld section, and locked-in stresses. The second type is a vertical crack which appeared at the longitudinal weld seam, apparently isolated, but which is essentially an extension of a crack in the sheet due to a stress raiser in the form of an existing hole.

The repairs made can be classified into three types. The first type, similar to the repairs made when the old extrusion was in place, consisted of cutting out the crack, welding the seam, and adding reinforcing plates. The second type involved cutting out the crack and rewelding the seam with a butt weld. In the third type a patch plate was inserted and butt welded after the area around the crack was removed. No repair of the first type was involved in a subsequent failure, whereas cracks did reappear in both of the other types of repair.

General Assessment of Cracks

All of the serious cracks that developed in the structure involved some sort of stress raiser which eventually led to distress under repeated load. The original stress raisers were the holes in the bottom extrusions. As the result of unsatisfactory repair of the cracks induced by these holes, new stress raisers were introduced, and these, coupled with poor weld penetration in some instances, resulted in the formation of still other cracks. In no case was a crack observed that was not due to one of these causes.

Fatigue Tests on Tension Specimens

Fig. 9 shows three laboratory specimens that were subjected to repeated load from approximately 9,000 psi to approximately 18,000 psi. This stress range corresponds roughly to dead load and dead load plus 2 times live load. The left-hand specimen, containing a $^1/_4$-in. drilled hole, underwent 380,000 cycles before it cracked. The results compare well with the history of crack number 1 although the cycling of the specimen was at a higher stress level. The middle specimen, which had a drilled hole reamed to $^1/_4$ in., underwent 890,000 cycles before cracking. The hole was then enlarged to $^1/_2$ in. and filled by welding, and the specimen underwent an additional 645,000 cycles before cracking. The specimen on the extreme right was drilled and reamed to $^1/_2$ in. After more than 2,000,000 cycles no crack was observed.

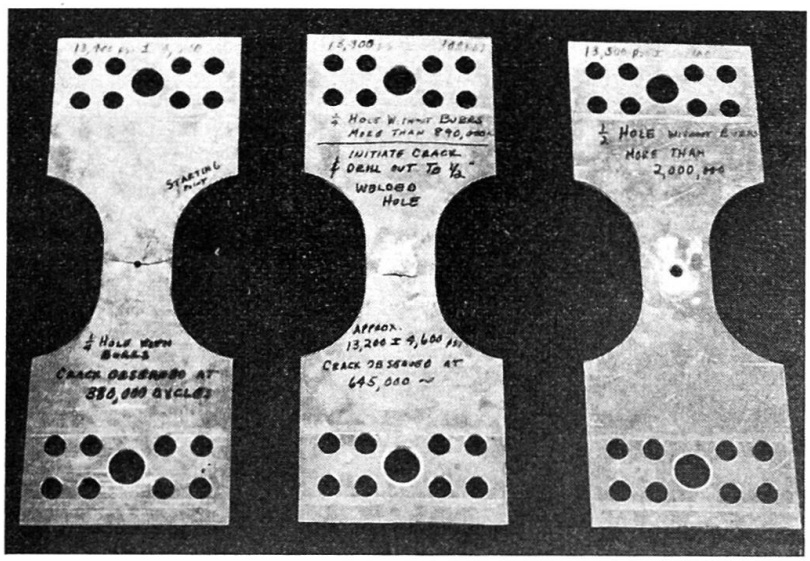

Fig. 9. Fatigue Specimens.

Experimental Determination of the Natural Frequency

A sack of sand, weighing approximately 75 lbs., was lifted 11 ft. above the center point of the bridge deck by a rope and pulley arrangement and then dropped. The resulting vertical vibrations were converted into electrical signals, amplified, and recorded on a paper strip recorder.

Based on the average of measured wave lengths and the known paper speed, it was found that the value of the natural frequency was 4.5 cycles per second, or 270 cycles per minute. For an idealized beam structure with flexural properties corresponding to those assumed for the bridge structure, the theoretical natural frequency is 5.1 cycles per second. The difference of approximately 12 percent is considered reasonable in view of the presence of damping, including the effect of restraint at the expansion end.

Summary

A welded aluminum prototype bridge was subjected to static and repeated load tests in order to determine its structural suitability for use on highways. No signs of distress, except for some local yielding and local buckling over the supports, were observed under static loads. The measured strains and deflections were in general what would be expected on the basis of theory.

The program of repeated-load tests included the application of 50,000 cycles at 1.0 times design moment, and 750,000 cycles at 1.5 times design moment. Before 448,000 cycles at 1.5 times design moment were completed, three cracks were discovered. All three cracks appeared to be due to the presence of holes drilled in the bottom extrusions to accommodate bolts which joined adjacent modules at their lower edges.

The first two cracks were repaired, but after the third crack the bottom extrusions were removed and replaced with others of a new design with all holes eliminated. Before the prescribed program of repeated-load tests was completed, six additional shutdowns were made in order to repair cracks. All of these cracks can be traced to the unsatisfactory repair of a previous crack or to holes that were present in the structure as erected.

Résumé

Un prototype de pont soudé en aluminium a été soumis à des essais de charge statiques et répétés, essais destinés à montrer si l'on pouvait utiliser de tels ouvrages sur les autoroutes. Aucun signe d'épuisement ne se montra lors des essais statiques, à part de légères déformations plastiques locales et un voilement local au droit des appuis. En général, les allongements et les flèches concordaient avec celles données par le calcul.

Le programme des essais à l'endurance comprenait 50000 cycles pour la sollicitation de service réglementaire puis 750000 cycles pour une sollicitation de 50% supérieure. Près du 448000e cycle de la seconde série, on découvrit trois fissures. Toutes ces fissures semblaient dues aux trous percés dans les profilés extrudés inférieurs, trous qui servaient à l'assemblage des éléments contigus à l'aide de boulons.

Les deux premières fissures furent réparées. A l'apparition de la troisième, on enleva les profilés inférieurs et on les remplaça par un nouveau profil sans trous. Avant d'atteindre le nombre de cycles prévu par le programme, les essais durent être interrompus six fois pour effectuer des réparations. Toutes ces fissures provenaient d'une réparation insuffisante des dommages précédents ou de trous percés dans l'ouvrage primitif.

Zusammenfassung

Um die bauliche Eignung einer geschweißten Aluminiumbrücke als Straßenbrücke zu analysieren, wurde diese statischer und wiederholter Belastung unterworfen. Abgesehen von leichten lokalen plastischen Formänderungen und örtlichem Ausknicken über den Auflagern, wurde unter ruhender Belastung kein Erschöpfungszeichen beobachtet. Im allgemeinen entsprachen die Formänderungen und die Durchbiegungen den theoretisch berechneten Werten.

Das Programm der Prüfung auf wiederholte Belastung umfaßte 50000 Lastwechsel unter dem 1,0-fachen Bemessungsmoment und 750000 Lastwechsel unter dem 1,5-fachen Bemessungsmoment. Vor dem Erreichen von 448000 Lastwechseln unter dem 1,5-fachen Bemessungsmoment wurden drei Risse entdeckt. Alle drei Sprünge schienen ihre Entstehung den Löchern in den unteren Strangpreßprofilen zu verdanken. In diesen Löchern waren die Bolzen eingesetzt, die die nebeneinanderliegenden Elemente verbanden.

Die ersten beiden Risse wurden repariert. Nach dem dritten Riß wurden die unteren Strangpreßgurte abgetrennt und durch ein neues Profil ohne Löcher ersetzt. Ehe das vorgesehene Lastwechselprogramm erfüllt war, mußte der Versuch noch 6mal zur Vornahme von Reparaturen unterbrochen werden. All diese neuen Risse konnten auf ungenügende Reparaturen der vorangegangenen Schäden oder auf Löcher in der ursprünglichen Konstruktion zurückgeführt werden.

Ia2

Fatigue Design and Endurance of Metal Structures

Calcul de la résistance à la fatigue des ouvrages métalliques

Ermüdungsberechnung und Dauerfestigkeit von Metallbauten

A. M. FREUDENTHAL
Columbia University, New York, N. Y.

In his General Report Professor Stüssi discusses the problem of the reduction of the endurance limit under random sequences of variable stress-amplitudes of a stress-spectrum including amplitudes below as well as above the conventional constant-amplitude endurance limit. On the basis of preliminary test-results performed to check the conclusion reached in my paper in the "Preliminary Publication" [1] that the stress-amplitudes below the conventional endurance limit produce significant damage because of their interaction with the stress-amplitudes above this limit, he attempts to show that this conclusion is not confirmed. He also suggests that the strain-hardening effect produced by high stress-amplitudes might be responsible for the specific and, as he says, "unexpected" test results reported in my paper. This latter suggestion is not convincing, as according to all evidence strain-hardening should be expected to raise the endurance limit rather than to lower it.

However, before discussing the points raised, particularly the discrepancy between Professor Stüssi's and my own test results, I should like to present new results of random-fatigue tests performed on a much more widely used metal than the SAE 4340 high-strength steel used in the first test series. The purpose of these tests was the same as that of the previously reported tests: to demonstrate that stress-amplitudes below the conventional endurance limit produce significant damage if mixed with a small number of stress-amplitudes above this limit, so that the design-significance of the endurance limit obtained in constant-amplitude tests is, at least, problematic.

The material used was ASTM-A-285 weldable mild carbon steel with nominal ultimate tensile strength $\sigma_u = 53{,}000$ psi, estimated conventional endurance

limit in bending $S_E = 28{,}000$ psi $= 0.53\ \sigma_u$ and yield limit in tension of 34,000 psi. The testing procedure is similar to that described in my paper in the "Preliminary Publication"; the stress-spectrum applied is exponential with respectively 0, 1, and 2 stress-amplitudes below the conventional endurance limit. Table I shows the actual test results in ascending order for the three stress-spectra applied; S_1 denotes the lowest, S_5, S_6 and S_7 the highest stress-amplitudes in terms of σ_u of the spectrum, p indicates the ratio of the lowest and of the highest stress-amplitude cycles in the total number of cycles applied. It should be noted that the nominal ultimate strength σ_u and the yield stress refer to uni-axial tension tests while the fatigue tests were performed in rotating bending; thus the maximum stress-amplitude applied of $0.95\ \sigma_u$ is, in fact, only slightly above the expected yield stress in bending which for round specimens is at least 40 percent above the yield stress in tension.

Table I. Number of Cycles to Failure in Thousands for ASTM-A-285 Steel Specimens under Randomized Exponential Load Distributions of Slope $h = 17.3$

	Spectrum No. 1	p	2	p	3	p
Spec.	$S_1 = 0.55$	0.82218	$S_1 = 0.45$	0.82200	$S_1 = 0.35$	0.822000
No.	$S_5 = 0.95$	0.00100	$S_6 = 0.95$	0.00018	$S_7 = 0.95$	0.000026
1	622.5		2,408.5		2,068.7	
2	646.3		2,743.0		3,879.7	
3	696.4		3,166.2		5,937.1	
4	816.5		4,356.9		6,497.4	
5	877.6		5,145.7		6,914.4	
6	971.4		5,747.0		7,076.0	
7	1,453.0		6,625.1		7,230.3	
8	1,705.4		7,606.4		8,055.1	
9	1,966.6		8,615.8		9,020.3	
10	2,019.5				9,342.3	
11					9,648.4	
12					9,871.9	
13					11,411.7	
14					20,111.0	
15					22,257.8	
V'_{OR}	1,294.0		5,827.7		10,561.0	
N'_{OR}	350.0		1,000.0		1,000.0	

The applied load spectra have identical slopes of 17.3 and identical highest stress-amplitudes $0.95\ \sigma_u$. They are therefore practically identical with Spectrum A (most severe) applied in the tests on SAE 4340 steel. They differ by their relation of the lowest stress amplitude S_1 to the conventional endurance limit $S_e = 0.53\ \sigma_u$. V'_{OR} and N'_{OR} denote, respectively, the "characteristic" life (probability level of failure $P = 1 - 1/e$) and the "minimum" life ($P = 0$) obtained by extreme value theory interpretation of test results [2].

The test results are evaluated in Table II which, in the last column, shows the effect, on the random fatigue life under the given stress-amplitude spectrum, of including or of not including stress-amplitudes below the conventional endurance limit. Thus the inclusion of two stress-levels below this limit reduces the fatigue life by a factor of almost four, which is of the same order of magnitude as that observed for the same spectrum on SAE 4340 steel.

Table II. Compensated Fatigue Life for ASTM-A-285 Steel Specimens for Tests with and without Inclusion of Stress Levels below the Endurance Limit $S_E = 0.53\ \sigma_u$

Spectrum No.	h	No. of stress levels below S_E	S_1	V'_R (mode) in thousands	Compensating factor	Compensated life (mode) in thousands
1	17.3	0	$0.55\,\sigma_u$	1,294	$1/(1-p_1-p_2) = 30.36$	39,932
2	17.3	1	0.45	5,828	$1/(1-p_1) = 5.62$	32,757
3	17.3	2	0.35	10,561	1.00	10,561

The results on ASTM-A-285 Steel therefore confirm the conclusions reached previously for SAE 4340 Steel: application of stress-levels below the conventional endurance limit produces significant fatigue damage. The damage is the more pronounced the larger the proportion of stress-amplitudes below this limit.

The key to the discrepancy between Professor Stüssi's and my own test-results is in this last conclusion, which confirms the trend established by the results on SAE 4340 Steel (there is a misplaced decimal point in the last figure of Spectrum C 1; the number should be 330.0 instead of 33.0). Damage at stress-amplitudes below the conventional endurance limit resulting from interaction with high stress-amplitudes becomes pronounced only when the damage directly produced by the latter is very small. When the variable-amplitude fatigue life is essentially determined by stress-amplitudes above the endurance limit, interaction effects become insignificant.

None of Professor Stüssi's test programs contains stress-amplitudes below the conventional endurance limit; the lowest amplitude of program I of $0.546\ \mathrm{t/cm^2}$ is practically *at* rather than *below* the endurance limit ($0.55\ \mathrm{t/cm^2}$). Thus the tests are not designed to discover possible damage *below* the endurance limit and are, in this respect, not really comparable to my own test. With respect to damage *at* the endurance limit by stress-amplitudes exceeding it, comparison of the mean values Δn for programs I and II seems to support Professor Stüssi's implied conclusion that no damage is produced *at* this limit: the sum of Δn for program I is $1684{,}1 \times 10^3$, while the sum of Δn for program II plus the (non-applied) number of cycles at $0.546\ \mathrm{t/cm^2}$ would be 1630.9×10^3 and thus clearly within the scatter-range of program I.

It should, however, be noted that in Professor Stüssi's tests the percentage of high stress-amplitudes is very high in comparison with my own tests: almost 18 percent of the stress-cycles are at the highest two amplitudes, producing directly roughly 86 percent of the total damage according to the linear damage law, compared to much less than 3 percent of stress cycles at these two amplitudes producing directly less than 2 to 5 percent of the total damage in my tests. Whatever damaging interaction effects between the high stress-amplitudes and the endurance limit might exist, they can hardly be noticeable when the fatigue life is essentially determined by the highest two stress-levels alone. The fact that the linear damage law is applicable in the interpretation of Professor Stüssi's tests shows, in fact, that stress-interaction effects are unobservable; this does not necessarily mean that they are non-existent, but only that Professor Stüssi's test programs have not been designed to bring these effects out. In all random fatigue tests performed at Columbia University in recent years it could be clearly shown that the linear damage law $\Sigma(\Delta n_i/n_i) = 1$ is approximately valid only when all stress-amplitudes are relatively high and fatigue lives relatively short ($\leqq 10^6$ cycles); the wider the range between the highest and lowest stress amplitudes and the smaller the percentage of the former, the larger the deviation from the linear law and the stronger the stress-interaction effect [3].

Professor Stüssi's statement in his General Report that my test results are not confirmed by his preliminary tests could therefore only be understood to mean that his specific test programs are not quite relevant to the purpose of my tests, and that therefore our results are not comparable. His results show as clearly that there are conditions under which the stress-interaction effect in fatigue is irrelevant, as mine show that there are other conditions under which this effect is highly significant. Our results are thus neither incompatible, nor does any difference between them prove anything beyond the fact that test-conditions have been sufficiently different to produce different results.

With respect to the test conditions it appears, however, that the exponential stress-amplitude spectra underlying my tests with their very small percentages of high amplitude stress cycles are closer to real conditions of structures under variable loads than the stress-programs selected by Professor Stüssi. In fact they have been derived from load records of airplane wings in operational flight. Therefore my conclusion that the constant-amplitude endurance limit is a fatigue design and performance characteristic of dubious value is not affected by the results of Professor Stüssi's tests.

References

1. A. M. Freudenthal, Prelim. Publication, Sixth Congress IABSE, Stockholm, 1960, p. 27—33.
2. A. M. Freudenthal and E. J. Gumbel, Advances in Applied Mechanics, vol. 4, p. 117, Academic Press, New York 1956.
3. A. M. Freudenthal and R. A. Heller, Journal Aeron. Sciences, vol. 26 (1959), p. 431—442.

Summary

On the basis of preliminary test-results performed to check the conclusion reached in the author's paper in the "Preliminary Publication" that the stress amplitudes below the conventional endurance limit produce significant damage because of their interaction with the stress-amplitudes above this limit, Professor Stüssi attempts to show that this conclusion is not confirmed. New results of random-fatigue tests performed on ASTM-A-285 weldable mild carbon steel confirm the conclusions reached previously for SAE 4340 Steel: Application of stress-levels below the conventional endurance limit produces significant fatigue damage.

The author states that his own tests and those of Professor Stüssi based on different specific test programs are not comparable.

Résumé

Se fondant sur les résultats d'essais préliminaires, effectués dans le but de contrôler les conclusions que l'auteur a avancées dans la «Publication Préliminaire» (conclusions indiquant que des contraintes d'amplitude inférieure à la résistance classique à la fatigue peuvent causer d'importants dommages, à cause de leur interaction avec des contraintes d'amplitude supérieure à cette limite) le Prof. Stüssi essaie de prouver que ces conclusions ne sont pas confirmées. Des nouveaux essais effectués sur l'acier doux, soudable ASTM-A-285 confirment les conclusions tirées des résultats obtenus pour l'acier SAE 4340 et qui sont: l'application de contraintes d'amplitude inférieure à la résistance classique à la fatigue cause d'importantes dégradations par fatigue.

L'auteur constate que ses résultats d'essais et ceux du professeur Stüssi ne peuvent pas être comparés par ce qu'ils se fondent sur des programmes spécifiques différents.

Zusammenfassung

Auf Grund von ersten Versuchsergebnissen zur Überprüfung der Schlußfolgerung, zu der der Autor in seinem Beitrag im «Vorbericht» gekommen ist,

daß nämlich Spannungsamplituden unterhalb der herkömmlichen Ermüdungsgrenze beträchtlichen Schaden anrichten wegen ihrer Wechselwirkung mit den Spannungsamplituden über dieser Grenze, versucht Prof. Stüßi zu zeigen, daß diese Schlußfolgerung nicht bestätigt wird. Neue Ergebnisse von Ermüdungsversuchen unter veränderlichen Spannungswerten, ausgeführt an schweißbarem, normalem Baustahl ASTM-A-285, sollen aber die früher gezogenen Schlußfolgerungen für SAE 4340-Stahl bestätigen: Anwendung von Spannungsstufen unter der konventionellen Dauerfestigkeitsgrenze ergeben einen bemerkenswerten Ermüdungsschaden.

Der Autor stellt fest, daß seine Versuchsresultate und diejenigen von Prof. Stüßi, die von verschiedenen spezifischen Versuchsprogrammen ausgehen, nicht vergleichbar sind.

Ia3

L'exploitation des séries de petite taille en résistance des matériaux

Die Interpretation der kleinen Serien in der Festigkeitslehre

The Interpretation of Small-sized Series in Strength of Materials

M. DAVIN
Laboratoire Central des Ponts et Chaussées, Paris

Parmi les problèmes fondamentaux qui conditionnent le dimensionnement des constructions, celui du «risque de défaillance locale», c'est-à-dire d'abaissement local de la résistance au-dessous du taux de contrainte subi en service, est un des plus importants.

Pour déterminer la forme des courbes de répartition en probabilité des résistances à la rupture, et rechercher les meilleures formules d'ajustement, nous avons, au Laboratoire Central des Ponts et Chaussées, réalisé des populations de forte taille (plusieurs centaines, même plusieurs milliers) aussi homogènes que possible, d'éprouvettes de mortier. Nous avons trouvé que la «loi de valeurs extrêmes»

$$F(x) = 1 - e^{-\left(\frac{x}{x_0}\right)^K}$$

(où x est la variable aléatoire représentant la résistance à la rupture et $F(x)$ sa fonction de répartition, x_0 et K des paramètres dépendant de la population considérée), permet pour les essais de compression ou de traction directe, des ajustements très satisfaisants de la partie inférieure de la courbe ($x < x_0$) la seule qui intéresse la sécurité des constructions. Pour la partie supérieure ($x > x_0$), cette formule représente moins bien la réalité, les courbes expérimentales étant plus étalées que les courbes théoriques. Ainsi, pour un écart quadratique moyen d'environ 8% correspondant à $K = 15$, une valeur supérieure de plus de 30% à la moyenne n'est pas, en fait, extrêmement exceptionnelle, alors que la formule lui attribue une probabilité inférieure à 10^{-13}, donc très inférieure à l'inverse du nombre total d'éprouvettes essayées dans tous les temps et dans tous les laboratoires du monde.

La série de forte taille a toutefois l'inconvénient de nécessiter une étude

spéciale, faite dans des conditions aussi particulières que possible, et il subsiste un doute quant à la possibilité d'en tirer des conclusions générales. C'est pourquoi nous avons recherché une méthode permettant d'exploiter les archives de notre Laboratoire, principalement composées de séries de taille 6 relatives à des essais de mortiers et bétons, notamment l'essai de compression sur cubes et l'essai de traction de Michaëlis.

Il faut bien comprendre que ces séries ne peuvent pas être considérées comme formant, par leur réunion, un échantillon de grande taille d'une «population mère» commune. En effet, les changements qui interviennent, d'une série à l'autre, sont principalement sous la dépendance de facteurs humains, à variations discontinues, le plus souvent rebelles aux lois statistiques: changement de l'opérateur ou perfectionnement de la technique d'essai en ce qui concerne le laboratoire; variations dans la provenance et la qualité du ciment, les spécifications officielles, progrès de l'industrie des liants hydrauliques; et même, transformation de la mentalité des ingénieurs qui demandent les essais, certains d'entre eux s'adressant systématiquement aux Laboratoires, d'autres n'y faisant appel que s'ils ont subi des mécomptes.

Nous les avons donc considérées comme appartenant à des populations toutes différentes, mais en raison de leur communauté de nature, nous avons admis que ces populations obéissent à des lois que l'on peut ramener à une formulation mathématique du type défini ci-dessous.

La fonction de répartition de la résistance pouvant toujours être représentée pour l'ensemble des populations considérées par:

$$F(x, \lambda, \mu, \nu \ldots)$$

$\lambda, \mu, \nu \ldots$ étant des paramètres qui varient d'une population à l'autre, nous admettons que cette fonction peut se mettre sous la forme:

$$F(x, \lambda, \mu, \nu) = \Phi[f(x, \lambda, \mu, \nu), g(x, \lambda, \mu, \nu) \ldots]$$

les f, g étant *très peu nombreux* et *très simples comme expression mathématique*. On aura par exemple:

$$F(x, \lambda, \mu) = \phi(\lambda x + \mu)$$

(deux paramètres, une seule fonction auxiliaire introduisant les paramètres sous forme linéaire).

Cette hypothèse est suggérée par l'examen des principales lois usuelles admises en statistique. La loi de Gauss, dans toute sa généralité, la 1ère loi de Pearson, quand on fixe les exposants p et q, la loi de valeurs extrêmes à variable non bornée inférieurement (dont la fonction de répartition est $F(x) = 1 - e^{-e^{\frac{x-x_0}{p}}}$), admettent précisément la formulation de l'exemple particulier ci-dessus. La loi de Galton, la loi de valeurs extrêmes du type défini plus haut comme meilleure loi d'ajustement des séries de grande taille (type à variable essentiellement positive) ont des fonctions de répartition du type

$$F(x, \lambda, \mu) = \phi(\lambda L(x) + \mu)$$

ou encore, si l'on fait le changement de fonction $\phi(L(\xi) = \Psi(\xi)$ et le changement de paramètre $\nu = e^{\mu}$.

$$F(x, \lambda, \nu) = \psi(\nu x^{\lambda}).$$

Si nous nous bornons au cas où il n'y a qu'une fonction auxiliaire, nous avons

$$F(x, \lambda, \mu, \nu \ldots) = \Phi[f(x, \lambda, \mu, \nu)];$$

f est supposée connue mais la fonction ϕ à une seule variable est supposée inconnue.

Si la taille n des échantillons est supérieure au nombre m des paramètres, la répartition, dans l'espace à n dimensions, des points P dont chacun figure un échantillon, nous donne une information sur la fonction Φ; mais cette information est plus facilement exploitable s'il est possible de trouver une famille de multiplicités (courbes, surfaces ou hypersurfaces) telle que la probabilité de présence du point P dans chaque portion d'espace délimitée par une ou plusieurs de ces multiplicités soit indépendante des paramètres.

Soit en particulier $f(x, \lambda, \mu) = \lambda x + \mu$. Nous considérons des échantillons de taille 3 et nous les représentons, dans l'espace à 3 dimensions, chacun par le point P dont les 3 coordonnées $x_1 x_2 x_3$ sont les 3 nombres constituant le résultat d'épreuve de l'échantillon. Si nous passons d'une population à une autre en changeant λ et μ, la figure de l'espace représentant la densité de probabilité de présence du point P subit, pour un changement de λ, une homothétie par rapport à l'origine, et pour un changement de μ une translation suivant la droite $D(x_1 = x_2 = x_3)$.

Donc si nous considérons un dièdre Δ formé par deux demi-plans passant par D, la probabilité de présence de P à l'intérieur de ce dièdre est la même pour tous les échantillons, et quand le nombre des échantillons croît indéfiniment, la proportion de points P à l'intérieur du dièdre converge en probabilité vers une valeur certaine égale à cette probabilité commune.

Si la loi étudiée est normale (loi de Laplace-Gauss) la «figure représentant la densité de probabilité de présence de P» pour un échantillon, est formée de sphères concentriques. En effet, cette densité est:

$$\frac{1}{(2\pi s^2)^{3/2}} e^{-\frac{(x_1-m)^2+(x_2-m)^2+(x_3-m)^2}{2s^2}}.$$

Donc la répartition entre les dièdres Δ est uniforme: si δ est la mesure en radians d'un tel dièdre, la proportion de points P à l'intérieur de Δ converge en probabilité vers $\frac{\delta}{2\pi}$.

En fait, des 3000 échantillons de taille 6 trouvés dans nos archives, nous avons tiré 60 000 échantillons de taille 3, en divisant chacun en deux parts des 10 manières possibles, et sur chacun des 60 000 nous avons considéré la quantité:

$$\theta = \pm \operatorname{Arc\,cos} \frac{2x_1 - x_2 - x_3}{2\sqrt{x_1^2 + x_2^2 + x_3^2 - x_1 x_2 - x_2 x_3 - x_3 x_1}}$$

(le signe devant Arc cos étant celui de $x_2 - x_3$) qui représente l'angle dièdre du plan passant par D et P avec le plan passant par D et l'axe des x_1. D'après ce qui précède, la répartition de θ tendrait vers l'uniformité entre $-\pi$ et $+\pi$, pour un nombre indéfiniment croissant d'échantillons, si les populations suivaient une loi normale.

Toutefois l'ordre des indices affectés à chacun des nombres formant l'échantillon doit être vraiment aléatoire, sans corrélation avec l'ordre de grandeur croissante ou décroissante. Or certains de nos résultats d'essais avaient été classés par ordre de grandeur; d'autres d'après l'ordre d'exécution des essais.

Nous avons donc commencé par opérer la permutation aléatoire systématique de nos échantillons, commandée par un procédé de randomisation.

Les nombres mis en œuvre, étant des résultats expérimentaux, étaient arrondis à la division du cadran la plus voisine de l'aiguille; d'où le risque d'un «biais» d'autant plus grave que les écarts entre x_1, x_2 et x_3 sont souvent de quelques divisions seulement. Nous avons corrigé ce biais, en ajoutant, à chacun des résultats bruts, une partie décimale définie elle aussi par un procédé de randomisation.

En définitive, c'était la répartition de θ entre des tranches égales (0 à 10°, 10° à 20° ...) qui nous intéressait. Pour économiser le temps de travail de la machine, nous n'avons pas, en réalité, calculé θ, mais seulement $\cos\theta$, c'est-à-dire la fraction algébrique en $x_1 x_2 x_3$, et nous avons étudié la répartition des valeurs trouvées entre les intervalles $\cos 0° - \cos 10°$, $\cos 10° - \cos 20°$, etc.

Le choix de tranches de 10° pour θ réalise un bon compromis entre deux exigences contraires: avoir assez de tranches pour obtenir une connaissance suffisante de la fonction représentant la distribution des points P par rapport à θ; avoir assez de points P dans chaque tranche pour réduire suffisamment les écarts relatifs accidentels.

Conformément à la théorie, notre courbe de fréquence admet, aux dits écarts près, la période $\frac{2\pi}{3}$. Les tranches ont des différences significatives qui prouvent l'existence d'écarts entre les lois des populations étudiées et la loi de Gauss. Les moins chargées sont celles voisines de $\pm 30°$, $\pm 90°$, $\pm 150°$. Les plus chargées sont celles voisines de $\pm 60°$ et de 180°; mais des maxima moins accusés existent au voisinage de 0° et $\pm 120°$.

Est-il possible de remonter de la fonction densité de probabilité en θ (supposée connue suffisamment par ces résultats) à la fonction $\phi(z)$ telle que $\phi(\lambda x + \mu)$ soit la forme générale de la fonction de répartition des populations étudiées? Ce problème comporte la résolution d'une équation intégrale non linéaire, qui peut en principe être obtenue, au moins numériquement, par une méthode de «cheminement fonctionnel». Considérons une «fonction de départ» ϕ_0 et la fonction $\chi_0(\theta)$ qui lui correspond (on la détermine par de simples quadratures). Etablissons alors entre χ_0 et χ un «trajet fonctionnel» c'est-à-

dire une famille de fonctions dépendant continûment d'un paramètre m et telle que pour $m=0$ on ait la fonction χ_0 et pour $m=1$ la fonction χ (le trajet sera «rectiligne» si la famille considérée est:

$$\chi_0 + m(\chi - \chi_0).$$

Déterminons de proche en proche les variations infiniment petites que doit subir Φ pour que les variations infiniment petites correspondantes de χ se situent sur le trajet fonctionnel: c'est un problème de Fredholm, et les calculatrices électroniques, qui opèrent facilement les inversions de matrices d'ordre élevé, peuvent généralement le résoudre numériquement avec une bonne approximation. Le cheminement permet donc d'arriver à une fonction Φ telle que la fonction qui lui corresponde soit χ (s'il n'est pas interrompu par des singularités). La principale difficulté paraît être le choix de la fonction de départ et la solution des indéterminations; le problème posé peut en effet admettre une infinité de solutions dont une seule est la bonne, il faut que la fonction de départ en soit assez voisine. Les études préalablement faites sur des séries de grande taille pourront guider ce choix.

Nos prétentions seront plus modestes car le travail mathématique serait trop considérable et la fonction $\chi(\theta)$ encore insuffisamment bien connue. Nous commençons par rechercher quelle serait la fonction $\chi(\theta)$ si l'on pose $\phi(\xi) = 1 - e^{-\left(\frac{\xi}{\xi_0}\right)^K}$ (loi de valeurs extrêmes).

La densité de probabilité dans le cas $\xi = x$ est

$$\varphi(x) = K \frac{x^{K-1}}{x_0^K} e^{-\left(\frac{x}{x_0}\right)^K} \quad \text{(en remplaçant } \xi_0 \text{ par } x_0)$$

et dans l'espace $x_1 x_2 x_3$ la densité de probabilité relative au point P

$$\varphi_P(x) = \frac{K^3 (x_1 x_2 x_3)^{K-1}}{x_0^{3K}} e^{-\left(\frac{x_1}{x_0}\right)^K - \left(\frac{x_2}{x_0}\right)^K - \left(\frac{x_3}{x_0}\right)^K}.$$

Dans chaque tranche θ à $\theta + d\theta$ nous commençons par intégrer entre les cônes $r = sz$ et $r = (s+ds)z$ avec

$$z = \frac{\sqrt{3}}{3}(x_1 + x_2 + x_3) \quad \text{et} \quad r = \sqrt{x_1^2 + x_2^2 + x_3^2 - z^2}.$$

Le volume élémentaire d'intégration est alors $z^2 s\, ds\, dz\, d\theta$. Si nous posons $x_i = m_i z$ avec $m_i = \frac{\sqrt{3}}{3}\left(1 + s\sqrt{2}\cos\left[\theta + \frac{2\pi}{3}(i-1)\right]\right)$ $(i = 1, 2 \text{ ou } 3)$ l'intégrale dans la tranche $d\theta$ est:

$$dI = d\theta \int_0^{s_l} \frac{K^3 (m_1 m_2 m_3)^{K-1}}{x_0^{3K}} s\, ds \int_0^{\infty} Z^{3K-1} e^{-\frac{(m_1^K + m_2^K + m_3^K) z^K}{x_0^K}} dz,$$

$$= 2\, d\theta\, K^2 \int_0^{s_l} \frac{(m_1 m_2 m_3)^{K-1}}{(m_1^K + m_2^K + m_3^K)^3} s\, ds.$$

(s_l étant la plus petite valeur positive de s qui annule l'un des m_i)

cette intégrale peut se calculer numériquement, en fonction de θ. On trouve, par exemple pour $K = 15$:

$$\frac{\chi(30°)}{\chi(0°)} = 1{,}172, \qquad \frac{\chi(60°)}{\chi(0°)} = 1{,}5075.$$

Aux lois de valeurs extrêmes correspondent des fonctions $\chi(\theta)$ qui présentent bien les maxima trouvés expérimentalement pour $\pm 60°$ et $180°$, mais non ceux trouvés pour $0°$ et $\pm 120°$. Cela tient à leur fort «étalement» du côté des faibles valeurs et à leur très faible étalement du côté des grandes valeurs.

Mais si on considère une loi symétrique qui se confond à peu près avec une loi de valeurs extrêmes pour les faibles valeurs de la variable, la fonction $\chi(\theta)$ correspondante a des maxima, tous égaux, pour $0°$, $\pm 60°$, $\pm 120°$, $\pm 180°$. En diminuant l'étalement du côté des grandes valeurs, on peut obtenir une fonction $\chi(\theta)$ conforme à notre répartition expérimentale (maxima principaux pour $\pm 60°$ et $180°$, et maxima moins accusés pour 0 et $\pm 120°$) tandis que la fonction $\phi(\xi)$ se rapproche des fonctions de répartition trouvées expérimentalement dans les séries de forte taille.

Pour tester l'application de lois de ce genre il eut été plus rationnel de considérer que les paramètres s'introduisent par l'intermédiaire de $\lambda L(x) + \mu$ ou de νx^{λ}, et, en conséquence, de remplacer, dans le calcul de θ, nos quantités $x_1 x_2 x_3$ par leurs logarithmes; mais cela représentait une augmentation importante du temps-machine, et comme les paramètres de dispersion de nos populations n'étaient pas eux-mêmes excessivement dispersés, cela n'aurait pas modifié beaucoup nos résultats: de plus il était intéressant de tester la loi normale.

Tableau du nombre de valeurs de θ tombant dans chaque classe

0	à	+ 10°	et	0	à	− 10°	3615
+ 10°	à	+ 20°	et	− 10°	à	− 20°	3440
+ 20°	à	+ 30°	et	− 20°	à	− 30°	3475
+ 30°	à	+ 40°	et	− 30°	à	− 40°	3430
+ 40°	à	+ 50°	et	− 40°	à	− 50°	3500
+ 50°	à	+ 60°	et	− 50°	à	− 60°	3715
+ 60°	à	+ 70°	et	− 60°	à	− 70°	3610
+ 70°	à	+ 80°	et	− 70°	à	− 80°	3510
+ 80°	à	+ 90°	et	− 80°	à	− 90°	3540
+ 90°	à	+ 100°	et	− 90°	à	− 100°	3320
+ 100°	à	+ 110°	et	− 100°	à	− 110°	3385
+ 110°	à	+ 120°	et	− 110°	à	− 120°	3485
+ 120°	à	+ 130°	et	− 120°	à	− 130°	3570
+ 130°	à	+ 140°	et	− 130°	à	− 140°	3450
+ 140°	à	+ 150°	et	− 140°	à	− 150°	3440
+ 150°	à	+ 160°	et	− 150°	à	− 160°	3375
+ 160°	à	+ 170°	et	− 160°	à	− 170°	3580
+ 170°	à	+ 180°	et	− 170°	à	− 180°	3680
							63120

Résumé

La fonction de distribution des résistances à la rupture d'une éprouvette d'un type donné, se détermine de préférence au moyen de séries de forte taille, mais les laboratoires disposent surtout, dans leurs archives, de séries de petite taille appartenant à des populations différentes mais de même nature.

Nous avons admis que la façon dont s'introduisent les paramètres dans la forme générale de la fonction est connue à priori et nous avons montré par un exemple tiré de 60 000 séries de taille 3 provenant du Laboratoire Central des Ponts et Chaussées, comment il est possible d'obtenir dans ces conditions une information sur cette forme générale.

Zusammenfassung

Die Verteilungsfunktion der Bruchfestigkeiten einer gegebenen Art von Probekörper bestimmt sich vorzugsweise mit Hilfe von großen Serien; leider verfügen die Laboratorien in ihren Archiven vor allen Dingen über kleine Serien, die verschiedenen Grundgesamtheiten gleicher Art angehören.

Wir haben angenommen, daß die Art, mit der sich die Parameter in die allgemeine Form der Funktion einführen, a priori bekannt sei und haben durch ein Beispiel mit 60 000 Serien der Größe 3 des «Laboratoire Central des Ponts et Chaussées» gezeigt, wie es möglich ist, unter diesen Umständen eine Auskunft über diese allgemeine Form zu erhalten.

Summary

The function of distribution of ultimate strength of a given pattern of test piece, is determined in preference by means of great sized series; but laboratories dispose especially in their files of small-sized series belonging to different populations of the same kind.

We have assumed that the way, by which parameters are introduced in the general form of the function, is known a priori, and we have shown, with an example from 60 000 series of size 3 from the "Laboratoire Central des Ponts et Chaussées", how it is possible under these conditions to obtain an information about that general form.

Leere Seite
Blank page
Page vide

Ia4

Discussion - Discussion - Diskussion

Shear Strength of Reinforced Concrete Beams Loaded Through Framed-in Cross-Beams (J. Taub, A. M. Neville, Ia6) [1])

Résistance à l'effort tranchant des poutres en béton armé chargées par l'intermédiaire de traverses (J. Taub, A. M. Neville, Ia6) [1])

Die Schubfestigkeit von Stahlbetonbalken mit Lastübertragung mittels Querbalken (J. Taub, A. M. Neville, Ia6) [1])

DONOVAN H. LEE
London

The shear strength of reinforced concrete beams covered by the tests described in the paper by Messrs. TAUB and NEVILLE should be considered as a rather special case because the beam has full moment at approximately the same point as nearly the full shear stress. High bond strength of the reinforcement in the main beam is therefore more advantageous than usual.

Another point on which the authors will no doubt agree is that tests of shear strength of isolated parts of a reinforced concrete structure must give optimistic results as compared with those same members in the complete structure. It seems to have been generally overlooked that beams forming part of a completed concrete framework will often be prevented from shrinkage by the rest of the structure and accordingly develop shrinkage stress corresponding to a fixed length condition. THOMAS [2]) gave long ago deduced shrinkage stress at early ages and the decay of stress for constant deformation was estimated by Building Research Station [3]) and also by Whitney in America some time ago. The maximum shear stress permitted on the concrete must

---

[1]) See "Preliminary Publication" — voir «Publication Préliminaire» — siehe «Vorbericht», p. 77.

[2]) Journ. Inst. Struct. Engrs. July 1936.

[3]) Journ. Inst. Struct. Engrs. Feb. 1933.

include allowance for the reduced strength caused by this shrinkage stress and not be based on tests of isolated beams.

By inference precast beams are largely unaffected. Also it is an interesting reflection that just as prestressing so greatly increases the shear strength rapid concreting of ordinary reinforced beams with inadequate freedom to shrink seriously reduces the resistance of the concrete to shear as one well known failure in North America seemed to confirm.

Of course many structures can shrink freely but for those that cannot sequences for the construction can easily be arranged so that the shear strength is not needlessly reduced by restraint to shrinkage.

Summary

The author discusses the shear strength tests described in the paper Ia6. He points out that the case considered is a rather special one because of maximum shear and bending stresses occurring nearly at the same section. Another point one must not overlook is that in effective structure the shear strength will often be reduced by shrinkage stresses and therefore these tests of isolated elements must give optimistic results.

Résumé

L'auteur discute les essais sur la résistance au cisaillement, dont traite la contribution Ia6. Il fait remarquer que le cas traité est plutôt une exception vu que les efforts tranchants et les tensions dues à la flexion sont maxima presque dans la même section.

De plus il ne faut pas oublier que la résistance au cisaillement d'ouvrages exécutés est souvent diminuée par les tensions dues au retrait. Il est donc clair qu'on obtiendra des résultats trop favorables lorsque les essais sont effectués sur des éléments isolés.

Zusammenfassung

Der Autor bespricht die Versuche über die Scherfestigkeit, die im Beitrag Ia6 enthalten sind. Er macht darauf aufmerksam, daß der behandelte Fall eher eine Ausnahme ist, da maximale Schub- und Biegespannungen fast im gleichen Schnitt auftreten.

Ein anderer Punkt, der nicht vergessen werden sollte, besteht darin, daß bei tatsächlichen Tragwerken die Scherfestigkeit oft durch Schwinden reduziert ist, so daß diese Versuche an isolierten Elementen eher optimistische Ergebnisse zeigen.